Structural changes of mullite precursors in presence of polyethyleneimine

E. Tkalcec *, D. Hoebbel, R. Nass, H. Schmidt

Institut für Neue Materialien, Im Stadtwald, Gebäude 43, D-66123 Saarbrücken, Germany

Received 26 November 1997; received in revised form 13 August 1998

Abstract

Thermal properties of two powders derived from the same calcined gel with a stoichiometric mullite composition (atomic ratio Al/Si = 3/1) wet milled in different solutions were studied by simultaneous differential thermal analysis, thermogravimetry and evolved gas analysis (DTA,TG,EGA, respectively), by density measurements and by ^{29}Si MAS NMR spectroscopy and X-ray diffraction (XRD). Calcined gel was milled either in ethanol or in ethanol with the addition of 0.03 g of polyethyleneimine (PEI) per gram of mullite. DTA, TG and mass spectrometry revealed esterification of unhydrated surface of particles formed by milling in ethanol. The difference in the structural evolution of powders and their dependence on annealing temperature seen in ^{29}Si MAS NMR spectra and XRD patterns is attributed to different degrees of segregation of alumina and silica components, and to differing compositions of transitory spinel phase. In both samples the segregation of silica and alumina was observed at temperatures less than that for mullite crystallization. The degree of segregation was much smaller in the sample milled in ethanol. Therefore, in the latter sample spinel with larger silica content incorporated in γ-Al_2O_3 will crystallize by annealing at 900°C, and Al-rich mullite at 1100°C. Due to greater segregation of silica and alumina component in the presence of PEI, the crystallization of spinel with smaller amounts of silica incorporated into γ-Al_2O_3 is shifted to 1100°C, and orthorhombic mullite to about 1200°C. The influence of PEI is indicated by a larger sintering density at lower temperatures.

1. Introduction

The high-temperature properties of mullite make it an attractive ceramic material for high-temperature insulating applications [1]. The applicability of mullite ceramics as substrates for multilayer computer packaging, photovoltaic energy transformers, and as infrared windows in the 3–5 μm wavelength region has recently gained considerable attention [2–4]. High-purity and ultra-fine mullite powders are important raw materials for these applications. The sol-gel process is a convenient method for synthesizing mullite precursors [5]. Depending on the starting materials and methods applied, the synthesized precursors have different properties, which in turn affect the resulting properties of the ceramics. The mechanism of mullite formation by the heating of gels is a function of their homogeneity. Therefore, considerable effort has been made to understand how the degree of mixing of the silica and alumina components is affected by the starting reagents and the reaction conditions [2,4–10].

* Corresponding author. Tel.: +49-681 9300 248; fax: +49-681 9300 223; e-mail: tkalcec@inm-gmbh.de

Different types of precursors have been identified on the basis of synthesis routes [6]. Some authors prefer to name their precursors after the method they employed, (slow hydrolysis, rapid hydrolysis method) [7], while others name them after the degree of homogeneity (single-phase, diphasic, hybrid) [8,9] or after the starting materials (polymeric, colloidal) [10]. According to Schneider et al. [11] three types of gel precursors can be identified. Type I precursors are the most homogeneous and amorphous below ~900°C. Above 900°C (long-time heat treatment) or at about 980°C (DTA conditions, 10 K/min) they crystallize to Al-rich mullite plus some coexisting amorphous SiO_2. Some segregation may also occur before crystallization in these types of precursors. In that case spinel (γ-Al_2O_3 or a solid solution of γ-Al_2O_3 and silica) crystallizes simultaneously with mullite. Type III precursors are also amorphous below 900°C but differ from type I in forming a spinel at 900°C plus non-crystalline SiO_2, while mullite formation follows at >1200°C. Type II precursors consist of alumina particles (boehmite, or pseudoboehmite) and amorphous SiO_2 in the as-prepared state. Transformation of boehmite or pseudoboehmite to γ-Al_2O_3 occurs at temperatures above 350°C, and mullite crystallization at about 1250°C.

One of the main concerns, that arises when sinter compacts are prepared from amorphous precursors is weight loss, which may occur at temperatures less than 600°C. Consequently sol-gel precursors have to be calcined at a temperature above 600°C. However, to use the advantage of greater reactivity during sintering, the calcination temperature should be less than that of mullite formation. The temperature required for mullite formation is ~1300°C for types II and III precursors and ~1000°C for type I precursors. However, the higher temperatures activate particle growth and the formation of agglomerates. Therefore, powders must be treated before shaping to eliminate agglomerates. Milling is usually considered to be a simple disintegrating process resulting in changes in the agglomerate and particle size distributions. However, in some cases it is possible to induce or speed up solid state reactions or reactions between the powder and the liquid used during a wet-milling operation [12,13].

To our knowledge, there are no data concerning the change of structure of amorphous mullite precursors during the wet-milling operation and its affect on subsequent mullite formation by heating. Therefore, the change of structure of type III powder during milling in ethanol (with and without addition of polyethyleneimine as dispersant), the path of mullite crystallization during subsequent heat treatment and the sintering behavior have been studied by ^{29}Si MAS NMR spectroscopy, differential thermal analysis (DTA), thermogravimetry (TG), evolved gas analysis (EGA), and by X-ray diffraction (XRD) analysis, as well as by density measurements.

2. Experimental procedure

Mullite precursor with Al/Si = 3/1 was prepared by dissolving aluminum nitrate in water. Tetraethoxysilane (TEOS) dissolved in ethanol was added dropwise to the nitrate solution under vigorous stirring. The molar ratio of H_2O/TEOS was kept at 13 : 1 to insure a more rapid hydrolysis [6] and crystallization of spinel at 980°C. The mixture was heated at 60°C under reflux conditions until gelation (8 days). The gel was dried at 120°C for 72 h and calcined at 700°C for 9 h. From the same calcined gel, D, two different powders were prepared, denoted as P and PP. For the preparation of sample P, the powder D was milled for 8 h in ethanol in an attrition mill with ZrO_2 balls. Precursor PP was prepared in the same manner, but 0.03 g of polyethyleneimine (PEI, MW = 600) per gram of mullite was added to the alcoholic solution by milling. Following the milling procedure the samples were dried at 120°C for 2 h. A flow chart of the powder synthesis is given in Fig. 1. The dried samples were compacted isostatically at 800 MPa, heated to a sintering temperature at the rate of 5 K min^{-1} and annealed at different sintering temperatures for 2 h. The sintered density of compacts was measured by the Archimedes method with distilled water as immersion liquid. The relative density was calculated using 3.26 g cm^{-3} for the average theoretical density of the heat-treated powder, since densities between 3.25 and 3.27 g cm^{-3} were obtained by

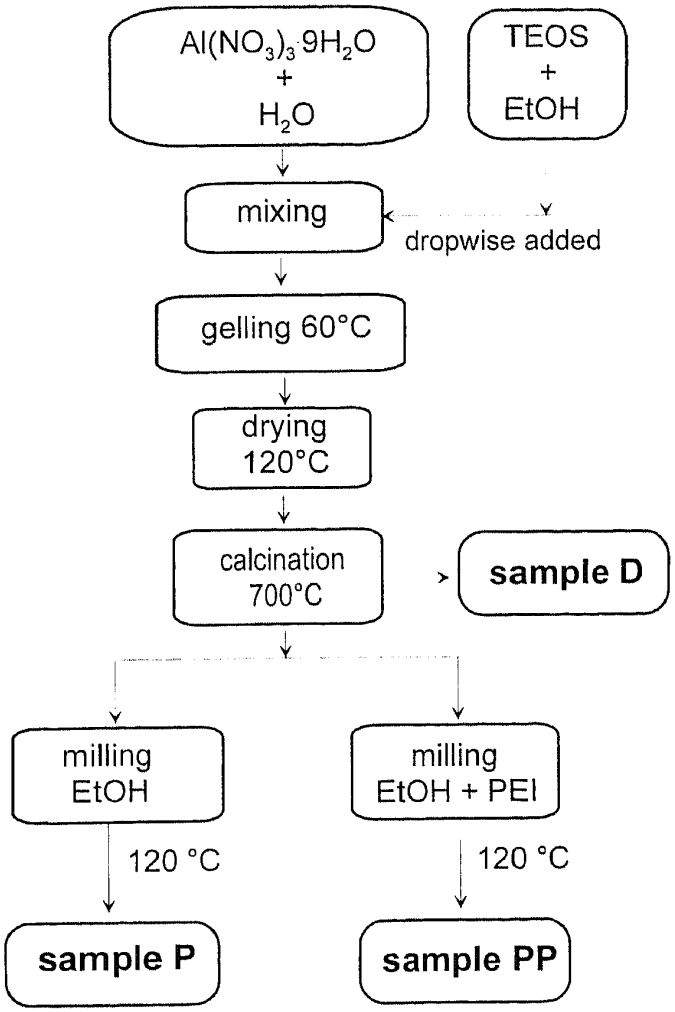

Fig. 1. Flow chart of powder synthesis.

measuring the densities of powder heat treated at 1650°C for 6 h. The density of the heat-treated powder is somewhat greater than that of pure mullite owing to the presence of ZrO_2, which entered the samples as wear debris from the milling media. This process was confirmed by chemical and XRD analysis [14]. The influence of ZrO_2 on the structure evolution of the powders during heat treatment is negligible and is therefore not taken into consideration in this study.

Simultaneous differential thermal analysis (DTA), thermogravimetry (TG) and evolved gas analysis (EGA) measurements were performed at the rate of 5 K min^{-1} under a constant oxygen flow of 75 cm^3 min^{-1} using a thermoanalyser (Netzsch STA/QMS 409/429-403) connected to a quadrupole mass spectrometer (Balzers QMG 420, 1-200 m/z). The gas analysis was performed in steps of 15 K. The weight of the samples was in all cases 0.1300 ± 0.002 g. The samples were contained in an Al_2O_3 sample holder, and an empty pan was used as a standard.

X-ray diffraction was carried out with a computer-controlled powder diffractometer (Siemens D500) using CuKα-radiation. Diffraction patterns were recorded from 5° to 70° 2θ in step-scan mode (10 s/0.02° 2θ). Si powder as an internal standard was used for determining the mullite lattice parameters. The content of Al_2O_3 in mullite was calculated from the relation between lattice parameter a and mullite composition, as given by Ban et al. [15].

Solid state ^{29}Si NMR spectra were obtained on a spectrometer operating at a field of 4.7 Tesla (Bruker MSL200). Acquisition parameters: $^{29}Si\{^1H\}$ single-pulse MAS experiment, rotation frequency: 3 kHz, pulse angle 3.3 μs (60°), repetition time 60 s. 12–24 h (720–1440 scans) accumulation time was necessary to achieve a reasonable signal-to-noise ratio in the spectra. The chemical shift is related to tetramethylsilane (secondary standard Q_8M_8 [16], M signal = 11.58 ppm). Cross-polarisation measurements could not be used owing to low proton concentration in the powders calcined at 700°C before milling. The samples for NMR investigations were brought stepwise to higher annealing temperatures of 700°C, 900°C, 1100°C, 1200°C and 1300°C at the rate of 5 K min^{-1} and held there for 2 h before cooling to room temperature. After each annealing step ^{29}Si MAS NMR spectroscopy and XRD were performed.

3. Results

3.1. Thermal analysis and sintering properties of the milled samples

The results of simultaneous DTA and TG analyses of the gel calcined at 700°C (sample D), the sample milled in ethanol and dried at 120°C (sample P), and the sample milled in ethanol with PEI addition (sample PP) are shown in Fig. 2. The DTA scan of sample D (Fig. 2(A)) has two exothermic maxima: a larger one at 981°C and a smaller one at around 1268°C. The same two

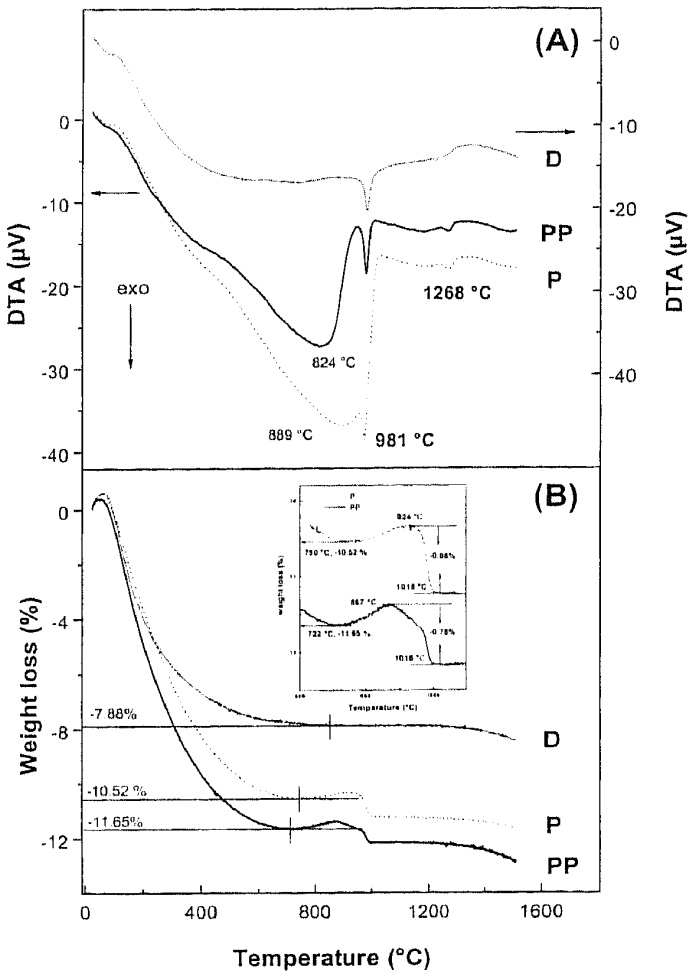

Fig. 2. (A) DTA and (B) TG curves of samples D, P and PP measured at a heating rate of 5 K min^{-1} in oxygen. The sample notation is explained in Fig. 1.

peaks are also observed in the milled samples. However, in a DTA scan of sample P an additional broader exothermic peak with maximum at about 889°C occurs. By addition of PEI into ethanol (sample PP) this peak becomes smaller and the maximum is shifted to 824°C. Whereas the peaks at 981°C and around 1268°C can be unambiguously ascribed to spinel and mullite formation, the peaks at 889°C and 824°C cannot be attributed to any crystalline phase, since there is no difference in XRD patterns of samples quenched from 700°C and 890°C. We attribute these DTA peaks to reaction products of the powders with the organic solvent (ethanol, or ethanol + PEI).

The TG curve of sample D (Fig. 2(B)) shows a monotonic weight loss from room temperature to 800°C. At 800°C the weight loss amounts to 7.88%, and between 800°C and 1500°C the sample lost an additional 0.83% of its weight. TG scans of the milled samples P and PP manifested a greater weight loss (−10.52% and −11.65% to 750°C and 722°C, respectively). Furthermore, both scans showed a weight increase in the region above 750°C and 722°C, respectively, followed by a smaller weight loss at about 1000°C. They are due to the oxidation of carbon and the escape of gaseous CO_2 from the sample. An enlarged plot of the TG curves in the interval 600–1000°C is given as an overlay in Fig. 2(B).

The mass spectra (MS) of H_2O ($m/z = 18$), CO_2 ($m/z = 44$) and H_2 ($m/z = 2$) evolved during DTA/TG analysis of the samples D, P and PP are shown in Fig. 3. The H_2O mass signal (Fig. 3(A))

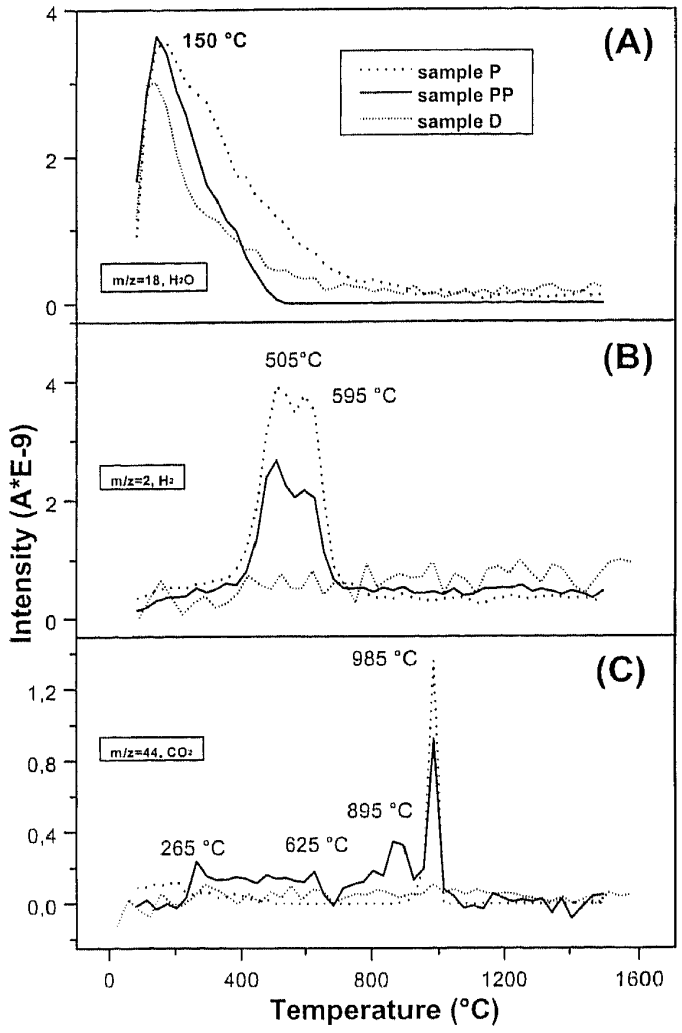

Fig. 3. Mass spectra of gases evolved during DTA/TG analysis in flowing oxygen. (A) intensity of $m/z(H_2O) = 18$; (B) intensity of $m/z(H_2) = 2$; and (C) intensity of $m/z(CO_2) = 44$. Heating rate: 5 K min^{-1}; oxygen flow 75 cm^3 min^{-1}. The sample notation is explained in Fig. 1.

observed at about 150°C is attributed to the release of molecular water from the samples. The subsequent progressive removal of hydroxyls from the calcined sample D and sample P milled in ethanol continues up to 900°C, whereas the H_2O mass signal of sample PP approaches zero at about 550°C. In the H_2 mass spectrum of the calcined sample D, no peak is recorded, whereas in the spectra of samples P and PP the peaks at 505°C and 595°C are observed (Fig. 3(B)). Similarly, the CO_2 mass spectrum of sample D (Fig. 3(C)) has no maximum. In the spectrum of sample P, a single signal at 985°C occurs, and in that of sample PP (milled in the presence of PEI) the same signal at 985°C and additional peaks at 265°C, 625°C and 895°C are observed (Fig. 3(C)). The mass spectra of H_2 and CO_2 will be discussed later.

Uniaxially pressed compacts of the samples were sintered at various temperatures. The sintered densities of compacts as a function of temperature are given in Fig. 4. PEI addition caused no increase in green density. However, its effect on the sintered density at 1400°C and 1500°C is larger.

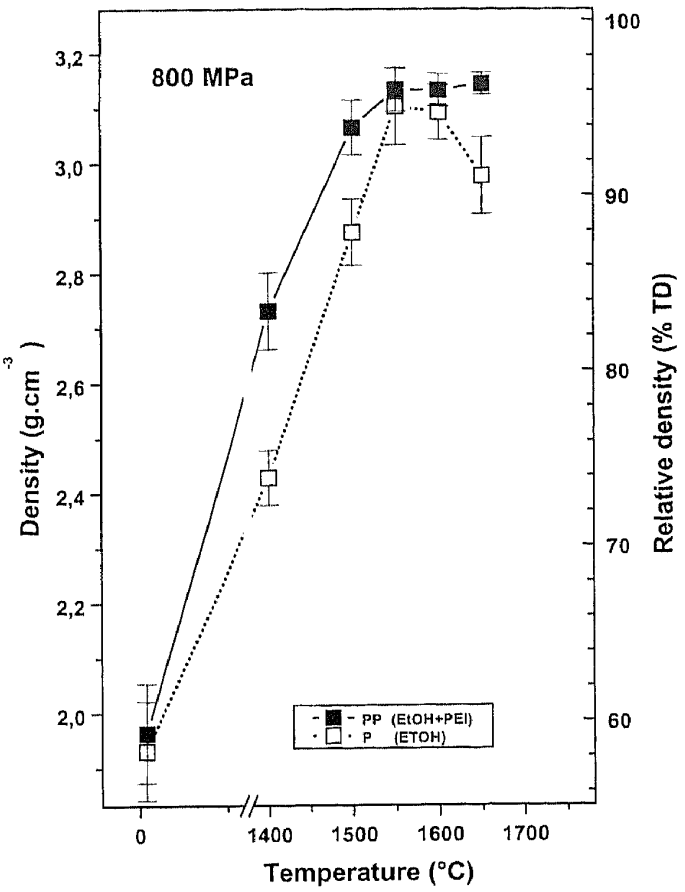

Fig. 4. Density as a function of sintering temperature. Specimen were isostatically pressed at 800 MPa and heated at a rate of 5 K min^{-1} to the sintering temperature. (-□-) milled in ethanol; (-■-) milled in ethanol with PEI. Holding time at each sintering temperature was 2 h. Lines are drawn as guides for the eye.

3.2. ^{29}Si NMR spectroscopy and X-ray diffraction analysis

It should be emphasized that due to overlap of the signals of Si atoms in Si–O–Si and Si–O–Al bonds in ^{29}Si NMR spectra [16] and to the width of the signals from amorphous aluminosilicates, only segregated, fully condensed silica with a chemical shift between −110 and −112 ppm can be assigned with certainty, while the assignment of other species is only an approximation. A fully condensed silicon atom connected via oxygen bridges to m Al atoms is labelled in this paper as $Q^4(m\text{Al})$, where m varies between 1 and 4, likewise a fully condensed silicon atom connected to four Si atoms is denoted as $Q^4(0\text{Al})$.

The ^{29}Si NMR spectra of calcined powder D and samples P and PP dried at 120°C are shown in Fig. 5. The spectrum of sample D displays one symmetrical signal with a chemical shift (δ) ranging between −85 and −105 ppm. According to the correlation of Engelhardt and Michel [16], the signal at −105 ppm is assigned to $Q^4(1\text{Al})$ units of a Si-rich aluminosilicate species, whereas that near −85 ppm results from Si atoms having four nearest Al neighbours, $Q^4(4\text{Al})$. The signals of $Q^4(m\text{Al})$ units with $m = 2$ and 3 are positioned between these two shifts. Additionally, chemical shifts of aluminum-free Q^2 and Q^3 [$(HO)_2Si(OSi)_2$ and $HOSi(OSi)_3$] units are also positioned in the range between −85 and −100 ppm [16]. Since the powder D was calcined at 700°C for 9 h, the dominance of Si–O–Al bonds is to be expected, while Al-free Q^2 and Q^3 units may be of subordinate influence. The spectrum is that of a homogeneous mixing of aluminum and silicon in the matrix. The spectrum of sample P (milled in ethanol and dried at 120°C) has an asymmetrical component with a maximum at about −105 ppm and a shoulder near −85 ppm, indicating some segregation of silica-rich aluminosilicate species from the matrix. The spectrum of sample PP (milled in ethanol with PEI addition and dried at 120°C) differs to a smaller extent from the spectrum

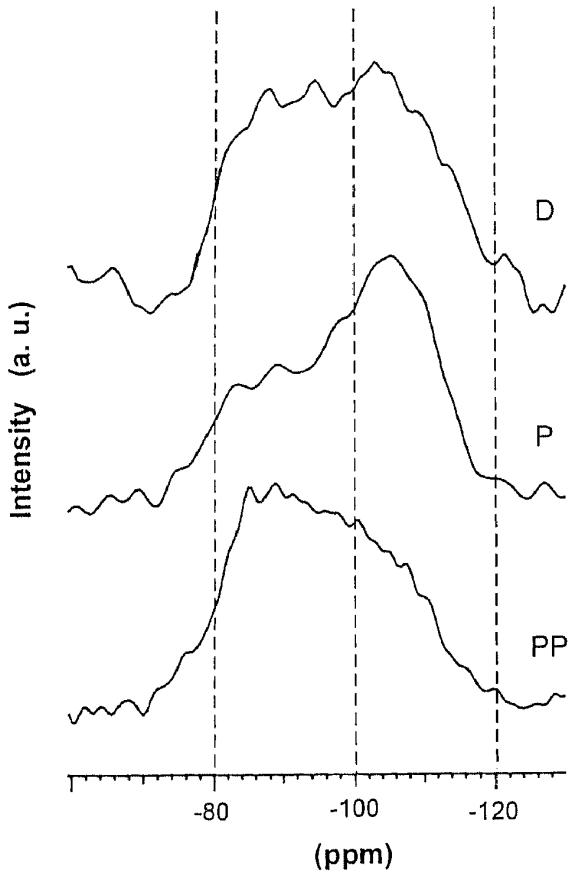

Fig. 5. ^{29}Si MAS NMR spectra of (D) gel calcined at 700°C, (P) calcined powder milled in ethanol and dried at 120°C, (PP) calcined powder milled in ethanol with PEI addition and dried at 120°C. Chemical shift is related to tetramethylsilane. The dashed lines are included as guides for the eye.

D, exhibiting an asymmetrical signal with a maximum around −85 ppm, which suggests a greater frequency of Si in Al-rich Q^4(4Al) environments and/or in Si(Al)–OR bonds (R = organics).

The spectra of the sample P annealed at various temperatures between 120°C and 1300°C are shown in Fig. 6. As mentioned above, the spectrum at 120°C indicates less homogeneous mixing of aluminum and silicon than that of the calcined powder D. The increase in annealing temperature induces further segregation of the Si-rich component, which is apparent in a shift of the intensity maximum at −105 ppm to larger fields, so that aluminium free Q^4(0Al) species with a chemical shift at −112 ppm (i.e. pure amorphous SiO_2) and aluminum-richer Q^4(3,2 Al) species with chemical shift in the range of −87 to −97 ppm are well resolved at 1100°C. By annealing at 1300°C, the component at −112 ppm disappears and only res-

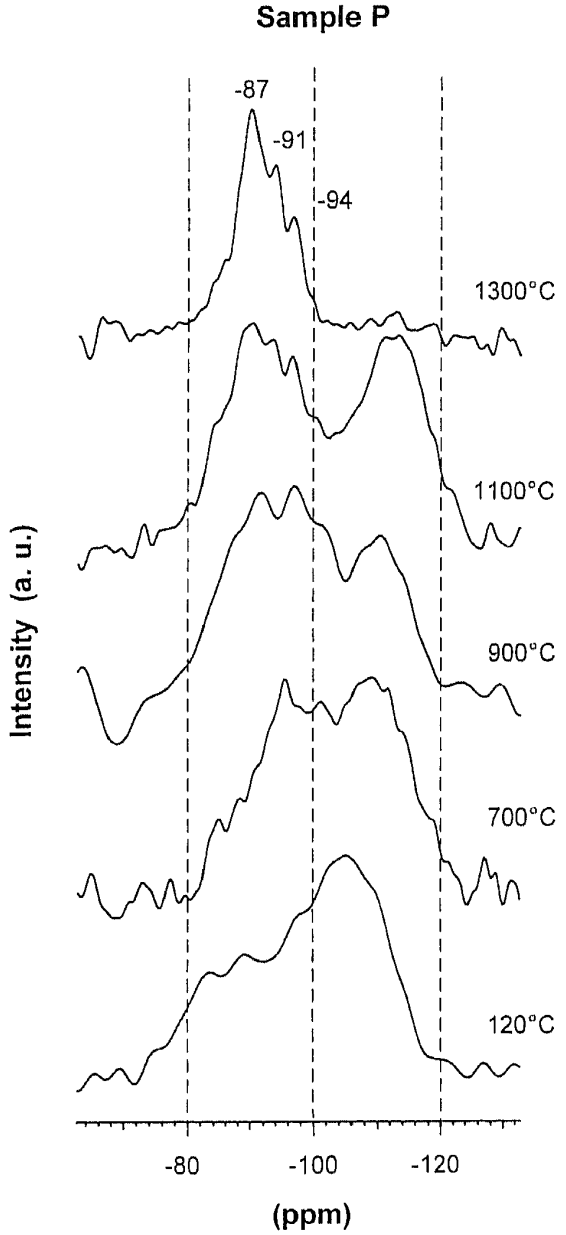

Fig. 6. ^{29}Si MAS NMR spectra of the sample P (milled in ethanol) and annealed at the specified temperatures for 2 h. Chemical shift is related to tetramethylsilane. The dashed lines are included as guides for the eye.

onances at −87, −91, and −94 ppm, with a shoulder at about −83 ppm attributed to mullite [17], are evident.

^{29}Si NMR spectra for the heat-treated sample PP are given in Fig. 7. The spectrum at 120°C is similar to that of the calcined powder D than rather that of sample P. The spectrum measured after annealing at 700°C (not shown in the figure) is broader and has a smaller signal-to-noise ratio than that measured at 120°C. At 900°C the dominance of the chemical shift at −106 ppm,

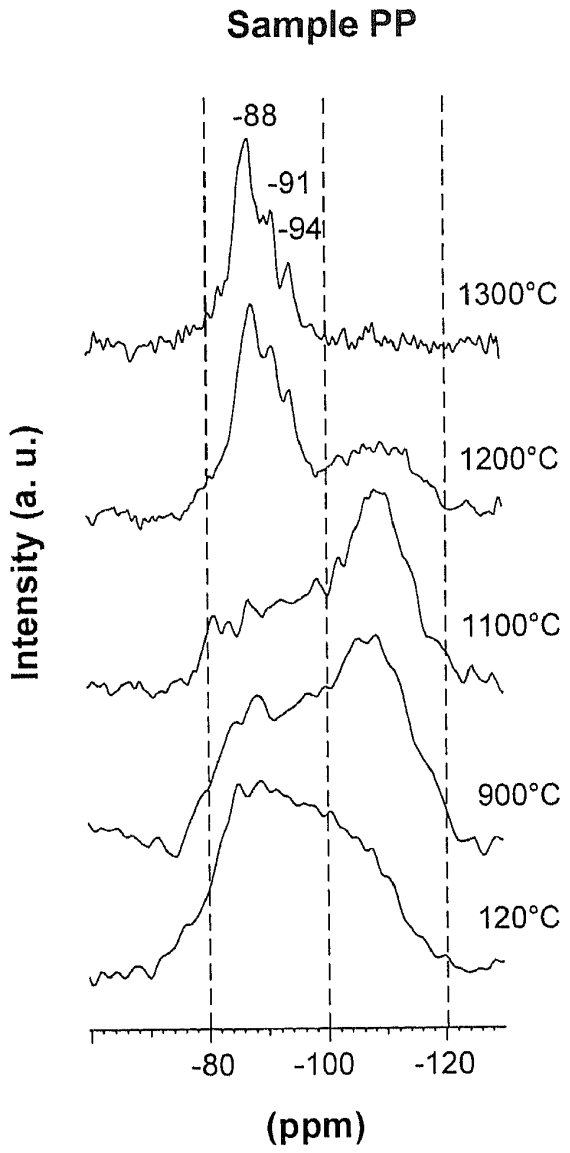

Fig. 7. ^{29}Si MAS NMR spectra of the sample PP (milled in ethanol+PEI solution) and annealed at the specified temperatures for 2 h. Chemical shift is related to tetramethylsilane. The dashed lines are included as guides for the eye.

typical for Si atoms in Si-rich environments (Q^4(1Al)), and a shoulder at −85 ppm, attributed to Si in Al-rich environments, are observed. With the increase in annealing temperature to 1100°C, the intensity of the Si-rich aluminosilicate component (−106 ppm) increases and its maximum is shifted to −112 ppm. The signal at −112 ppm (pure amorphous silica) decreases in amplitude at higher temperatures as a result of mullite crystallization, so that at 1200°C a smaller amount of free SiO_2 and at 1300°C no free SiO_2 is detected. The resonances at −88, −91 and −94 ppm are again attributed to crystalline mullite [17].

The XRD patterns of mullite precursors annealed at different temperatures are given in Fig. 8(A) and (B). The figures show the angular region of 2θ from 24° to 27°, which contains the most intense lines (120) and (210) of mullite, and the 2θ region from 44° to 49°, where the second most intense (400) line of spinel occurs. Powder P annealed at 700°C for 2 h is still amorphous (Fig. 8(A)). Spinel as the main phase and a trace of mullite were found in the sample annealed at 900°C. Pseudotetragonal, Al-rich mullite becomes the major phase at 1100°C, while the amount of spinel is reduced. The lattice parameters of pseudotetragonal Al-rich mullite at 1100°C are $a=$ 0.7612(7) nm, $b=0.7675(3)$ nm and $c=0.28814(9)$ nm [1]. At 1300°C, orthorhombic mullite is formed with the following lattice parameters: $a=0.7571(2)$ nm, $b=0.7685(1)$ nm and $c=0.28864(4)$ nm.

Fig. 8(B) shows the X-ray diffraction analysis of the heat-treated sample, PP. The sample annealed at 900°C contains much less spinel than the sample P annealed at the same temperature. No a trace of mullite was observed in the former at 900°C. Even at 1100°C, where the maximum intensity of the spinel phase is obtained, no mullite was observed. Following heat treatment at 1200°C the spinel is nearly completely consumed and orthorhombic mullite with lattice parameters $a=0.7572(1)$ nm, $b=0.7688(1)$ nm and $c=0.28857(3)$ nm is found. At 1300°C orthorhombic mullite with nearly the same lattice constants ($a=0.7569(2)$ nm, $b=$ 0.7687(1) nm and $c=0.28859(3)$ nm) was observed.

4. Discussion

4.1. Thermal analysis and sintering behaviour

The synthesis route used in this work (Fig. 1) leads to the formation of an amorphous mullite precursor, which can be designated as a type III precursor according to the definition of Schneider

[1] Numbers in parentheses correspond to standard deviations in the last digit quoted.

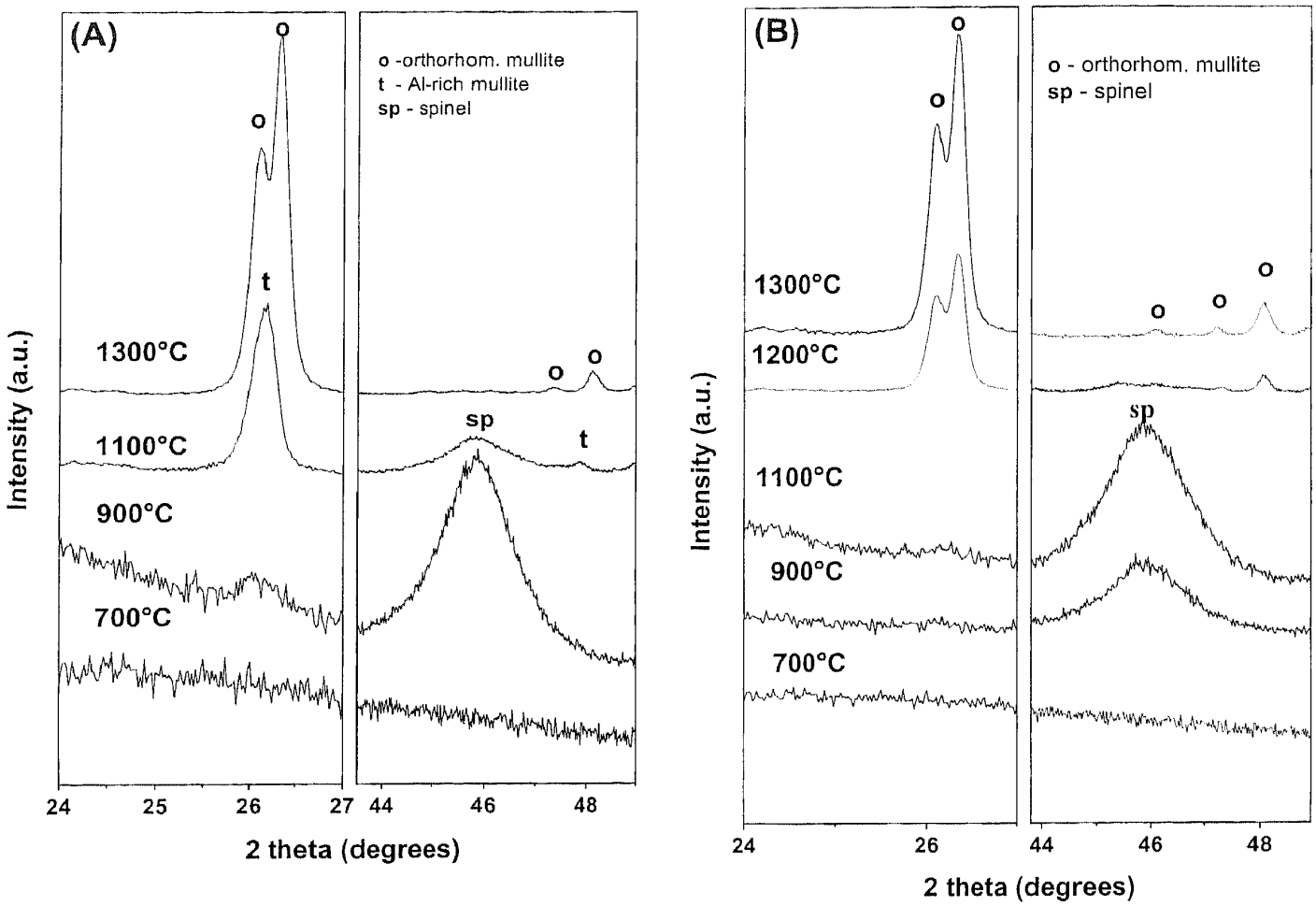

Fig. 8. XRD patterns of (A) sample P, (B) sample PP. The angular region of 2θ from 24° to 27°, containing the most intense lines (120) and (210) of mullite, and the 2θ region from 44° to 49°, where the second most intense (400) line of spinel appears, are presented in both diagrams.

et al. [11]. This type of precursor has two exothermic peaks in DTA scans (Fig. 2(A)). The first peak corresponds to crystallization of spinel (γ-Al_2O_3 or a solid solution of γ-Al_2O_3 and SiO_2), which later transforms into mullite, thus causing the second exothermic peak at around 1268°C. Calcination at 700°C even for 9 h does not bring about the complete dehydration/dehydroxylation of the sample, as shown by simultaneous TG/MS analyses of the calcined powder D (Figs. 2 and 3).

Grinding particles in ethanol for 8 h apparently causes cleavage of Si(Al)–O–Si bonds (either by alcoholysis and/or mechanically induced), the esterification of Si(Al)–O^- and the formation of Si(Al)–OR ($R = C_2H_5$) units. The latter decompose during thermal analysis in flowing oxygen, evolving the gaseous products measured by mass spectrometry (Fig. 3(B) and (C)). The signals at 505°C and 595°C in the H_2 ($m/z = 2$) mass spectra (Fig. 3(B)) of samples P and PP are attributed to the cleavage of C–H bonds in Si(Al)–O–C_2H_5 units, in accordance with Belot et al. [18]. However, a higher temperature is needed to induce the cleavage of C–O bonds and the oxidation of carbon. The small weight increase followed by a small decrease at about 1000°C in TG scans of milled samples (overlay in Fig. 2(B)) is evidence for the oxidation of carbon and the escape of gaseous CO_2. MacKenzie et al. [19] found that organic residuals originating from by-products of the gels derived from TEOS and Al sec-butoxide are thermally stable under dynamic conditions to at least 900°C. They also assumed that carbon is one of intermediate degradation products of organic residuals. The same authors emphasized that the presence of carbon could influence the structural evolution of the gel during heating.

The organic residuals originating from the degradation of polyethyleneimine are stable to heat treatment to about 895°C (as seen in the MS spectra of CO_2 in Fig. 3). Further investigations are needed to answer the question of how polyethyleneimine molecules are anchored to the surfaces of the particles. However, the DTA/TG/MS results suggest that a chemical bond probably exists between PEI and the unhydrated Si(Al)–O^- surfaces formed by grinding. The conclusion that esterification decreases in the presence of PEI is supported by the intensity signals of the H_2 mass spectra and by the peak at 985°C in the CO_2 mass spectra (Fig. 3).

The results of the density measurements show an affect of PEI on the pressureless sintering of mullite precursors (Fig. 4). The degree of densification of compacts with PEI addition is larger than that without PEI over the entire temperature range. The largest effect occurs at sinter temperatures of 1400°C and 1500°C. The influence of PEI is explained by the larger segregation of SiO_2 and of the Al_2O_3 component in the sample during thermal treatment, which induces reaction sintering in the presence of the liquid SiO_2 phase. It is well known that, in the early stages of reaction sintering, the presence of a liquid phase has a decisive affect on sintering. Kanka and Schneider [20] observed that liquid phase sintering at stoichiometrical mullite compositions produces relatively large prismatic mullite crystals embedded in a fine grain matrix, which we have also confirmed by SEM analysis [14].

4.2. ^{29}Si NMR spectra and XRD patterns

The ^{29}Si NMR spectrum of the calcined sample D (Fig. 5) shows a distribution of silicon sites representative of a homogeneous mixing of aluminum and silicon. The same homogeneous mixing of silicon and aluminum has been observed by Gerardin et al. [21] and Schneider et al. [4] in the same type of mullite precursors. Taking into the consideration the fact that powder D was calcined at 700°C for 9 h, the dominance of $Q^4(m\text{Al})$ species with $m = 1$–4 is to be expected. However, the presence of Si(Al)–OH bonds should not be ignored, since the weight loss in the TG scan amounts to 7.88%, and predominantly H_2O was evolved by thermal analysis (Figs. 2 and 3). The asymmetry of the spectrum of sample P (milled in ethanol and dried at 120°C) could be understood as an increase of the condensation degree of Si–O bonds [19]. The higher condensation degree of Si atoms resulted either from condensation reactions of Si–OH and Si–OC_2H_5 units (the latter are formed by reaction of ethanol with Si–OH) or from Si–O–Al bonds containing species which undergo alcoholysis followed by homo-condensation reactions [22]. The ^{29}Si NMR spectrum of the sample annealed at 700°C (Fig. 6) shows a slight shift of the signal's center of gravity to larger field, which corresponds to a larger averaged condensation degree of Si-containing species. However, the width of the ^{29}Si NMR signal still indicates a distribution of different structural Si(Al)–O units, and the sample is still amorphous. At 900°C, the greatest amount of silicon is located in Al-rich environments, $Q^4(m\text{Al})$ $m = 4$, 3, 2, and the lesser amount in pure silicon surroundings. The chemical shift at −112 ppm related to silicon in $Q^4(0\text{Al})$ units (pure SiO_2 phase) and the shifts in the range of −87 to −94 ppm, attributed to Si-sites in aluminosilicates like mullite [21,23], are well resolved at 1100°C, though the features of the latter are broader than for fully crystalline mullite. The increase in the amount of Si atoms in pure silicon environments at 1100°C is explained by crystallization of Al-rich mullite, during which some amorphous silica is always expelled [17,21]. The latter is progressively reincorporated into the mullite lattice with increasing temperature, as shown by absence of the $Q^4(0\text{Al})$ signal in the sample annealed at 1300°C. The presence of poorly crystallized spinel phase was observed by XRD analysis (Fig. 8(A)) at 900°C. Because of the width of the spinel phase's peaks, it is difficult to identify this phase as γ-alumina or as γ-Al_2O_3 solid solution. Pseudotetragonal, Al-rich mullite and some spinel were observed at 1100°C and orthorhombic mullite at 1300°C. The chemical composition of mullite deduced from the relationship between the lattice parameter a and the Al_2O_3 content [15] was found to be 72 mol% Al_2O_3 (Al/Si = 5.2) at 1100°C and 64.8 mol% Al_2O_3 (Al/Si = 3.68) at 1300°C. With a further

increase in temperature, the alumina-rich composition gradually shifts towards the expected Al/Si = 3/1 ratio. At 1600°C orthorhombic mullite with 61.8 mol% Al_2O_3 (Al/Si = 3.23) was observed. No corundum was detected at any temperature.

The structural evolution and formation of crystalline phases in sample PP (Figs. 7 and 8(B)) is quite different from those of sample P. We suggest that the ^{29}Si NMR at 120°C indicates the predominance of Al-rich Q^4 (4Al) [21] and of Si(Al)–OR species [19], owing to the reaction of particle surfaces with PEI/ethanol. Structural rearrangement by condensation reactions is seen at 700°C (the spectrum is not given here). At 900°C, Q^4(0Al) species (amorphous silica) dominate, and fewer Si–O–Al units are found. The dominance of Q^4(0Al) species is enhanced at 1100°C, at which the maximum amount of spinel is observed in the XRD pattern. The decrease in the amount of amorphous silica above 1100°C reflects its reaction with spinel forming orthorhombic mullite with 64.8 mol% Al_2O_3 (Al/Si = 3.68) at 1200°C. The composition of mullite remains nearly constant in the temperature range between 1200°C and 1300°C.

Regarding the results of ^{29}Si NMR spectroscopy and XRD analysis it can be stated that differences in the milling liquid have an affect on the formation of phases by thermal treatment. The segregation of pure silica before crystallization of mullite is evident in both samples, but it is smaller in the sample milled in ethanol (sample P). Therefore, it is reasonable to assume that spinel with a larger silica content will crystallize in sample P annealed at 900°C. The smaller diffusion distances between Al and Si enable crystallization of pseudotetragonal Al-rich mullite (72 mol% Al_2O_3) at 1100°C, which then transforms by reacting with amorphous silica to form orthorhombic mullite. When PEI is added to ethanol, the segregation of SiO_2 and Al_2O_3 is greater, and the crystallization of spinel with a smaller amount of silica incorporated into γ-Al_2O_3 occurs at 1100°C. The displacement of spinel crystallization to higher temperature results in the shift of the crystallization temperature of orthorhombic mullite (64.8 mol% Al_2O_3) to 1200°C.

The composition of the spinel phase has been a point of controversy in the literature, with proposed compositions varying between 0 and 20 mol% of SiO_2 [21,24,25]. The results here suggest an explanation for the disagreements found in literature regarding the composition of spinel crystallized at 980°C. The composition of spinel could depend not only on temperature, as observed by Schneider et al. [25], but also on the presence of organics in the sample. MacKenzie et al. [19] proposed an affect of organics on the structural evolution of the gel, but they did not define this affect. Further, our results suggest that PEI increases the segregation of silica and alumina components, consequently affecting the composition of spinel and finally the crystallization temperature of mullite in the Al_2O_3–SiO_2 system.

5. Conclusion

Simultaneous DTA/TG analysis and mass spectrometry (MS) unambiguously proved that amorphous mullite precursors reacted with ethanol used as milling liquid, forming non-bridged Si(Al)–OR bonds ($R = C_2H_5$). The pyrolysis of the Si(Al)–OR groups in oxidizing atmosphere extends to gel crystallization at ~980°C. Polyethyleneimine (PEI) added as a dispersant decomposes completely at 895°C.

The ^{29}Si NMR spectra showed difference in the structural evolution of amorphous precursors induced by milling in ethanol or in ethanol with PEI. The induced structural differences resulted in different temperatures of spinel and mullite crystallization. In both samples the segregation of silica and alumina was observed in the amorphous state; however, it was much higher when polyethyleneimine (as a dispersant) was added to the milling liquid. Therefore, in powder milled in ethanol, spinel crystallized upon annealing at 900°C and mullite at about 1100°C, whereas in the presence of PEI spinel crystallization was shifted to 1100°C and that of mullite to 1200°C.

This difference in the crystallization path of mullite is indicated by the sintering properties of the samples. Larger sintering density is obtained over the entire temperature range with the

addition of PEI, due to the larger amount of liquid SiO_2 phase. The largest increase in density is seen at 1400°C and 1500°C.

Acknowledgements

The authors acknowledge Dipl. Chem. M. Nacken for support in performing the NMR measurements.

References

[1] S. Somiya, Y. Hirata, Am. Ceram. Soc. Bull. 70 (1991) 1624.
[2] M.D. Sacks, H. Lee, J.A. Pask, in: S. Somiya, R.F. Davis, J.A. Pask (Eds.), Ceramic Transactions, vol. 6, Mullite and Mullite Matrix Composites, Am. Ceram. Soc., Westerville, OH, 1990, p. 167.
[3] I.A. Aksay, D.M. Dabbs, M. Sarikaya, J. Am. Ceram. Soc. 74 (1991) 2343.
[4] H. Schneider, K. Okada, J. Pask, Mullite and Mullite Ceramics, Wiley, Chichester, 1994, pp. 105–140.
[5] H. Schneider, D. Voll, B. Saruhan, J. Sanz, G. Schrader, C. Rüscher, A. Mosset, J. Non-Cryst. Solids 178 (1994) 262.
[6] K. Okada, N. Otsuka, in: S. Somiya, R.F. Davis, J.A. Pask (Eds.), Ceramic Transactions, vol. 6, Mullite and Mullite Matrix Composites, Am. Ceram. Soc., Westerville, OH, 1990, p. 375.
[7] K. Okada, N. Otsuka, J. Am. Ceram. Soc. 69 (1986) 652.
[8] D.W. Hoffmann, R. Roy, S. Komarneni, J. Am. Ceram. Soc. 67 (1986) 468.
[9] J.C. Huling, G.L. Messing, J. Am. Ceram. Soc. 74 (1991) 2374.
[10] B.E. Yoldas, in: S. Somiya, R.F. Davis, J.A. Pask (Eds.), Ceramic Transactions, vol. 6, Mullite and Mullite Matrix Composites, Am. Ceram. Soc., Westerville, OH, 1990, p. 255.
[11] H. Schneider, B. Saruhan, D. Voll, L. Mervin, A. Sebald, J. Eur. Ceram. Soc. 11 (1993) 87.
[12] F.W. Dynys, J.W. Halloran, J. Am. Ceram. Soc. 64 (1981) C-62.
[13] D.E. Niesz, R.B. Benett, in: L.L. Hench, G.Y. Onoda, Ceramic Processing Before Firing, chap. 7, Wiley, New York, 1978, p. 61.
[14] E. Tkalcec, R. Nass, T. Krajewski, R. Rein, H. Schmidt, J. Eur. Ceram. Soc. 18 (1998) 1089.
[15] T. Ban, K. Okada, J. Am. Ceram. Soc. 75 (1992) 227.
[16] G. Engelhardt, D. Michel, High Resolution Solid-state NMR of Silicates and Zeolites, Wiley, New York, 1987, p. 143.
[17] I. Jaymes, A. Douy, D. Massiot, J.P. Coutures, J. Non-Cryst. Solids 204 (1996) 125.
[18] V. Belot, R.J.P. Corriu, D. Leclercq, P.H. Mutin, A. Vioux, J. Non-Cryst. Solids 147&148 (1992) 52.
[19] K.J.D. MacKenzie, R.H. Meinhold, J.E. Patterson, H. Schneider, M. Schmüker, D. Voll, J. Eur. Ceram. Soc. 16 (1996) 1299.
[20] B. Kanka, H. Schneider, J. Mater. Sci. 29 (1994) 1239.
[21] C. Gerardin, S. Sundaresan, J. Benziger, A. Navrotsky, Chem. Mater. 6 (1994) 160.
[22] C.J. Brinker, G.W. Scherer, Sol–Gel Science, The Physics and Chemistry of Sol–Gel Processing, Academic Press, San Diego, 1990, pp. 108–229.
[23] I. Jaymes, A. Douy, D. Massiot, J.P. Coutures, J. Mater. Sci. 31 (1996) 4581.
[24] H. Schneider, L. Mervin, A. Sebald, J. Mater. Sci. 27 (1992) 805.
[25] H. Schneider, D. Voll, B. Saruhan, M. Schmücker, T. Schaller, A. Sebald, J. Eur. Ceram. Soc. 13 (1994) 441.